electrochem

MDPI

Article

Co-Electrodeposition of Au–TiO_2 Nanocomposite and the Micro-Mechanical Properties

Yu-An Chien [1], Tso-Fu Mark Chang [1,*], Chun-Yi Chen [1], Daisuke Yamane [2], Hiroyuki Ito [1], Katsuyuki Machida [1], Kazuya Masu [1] and Masato Sone [1]

1 Institute of Innovative Research, Tokyo Institute of Technology, 4259 Nagatsuta-cho, Midori-ku, Yokohama, Kanagawa 226-8503, Japan; chien.y.aa@m.titech.ac.jp (Y.-A.C.); chen.c.ac@m.titech.ac.jp (C.-Y.C.); ito.h.ah@m.titech.ac.jp (H.I.); machida.k.ad@m.titech.ac.jp (K.M.); masu.k.aa@m.titech.ac.jp (K.M.); sone.m.aa@m.titech.ac.jp (M.S.)

2 Department of Mechanical Engineering, Ritsumeikan University, 1-1-1 Noji-Higashi, Kusatsu, Shiga 525-8577, Japan; dyamane@fc.ritsumei.ac.jp

* Correspondence: chang.m.aa@m.titech.ac.jp

Received: 14 September 2020; Accepted: 29 October 2020; Published: 1 November 2020

Abstract: Strengthening of electrodeposited Au-based materials is achieved by co-electrodeposition with TiO_2 nanoparticles dispersed in a sulfide-based gold electrolyte. TiO_2 content in the composite film is adjusted by concentration of the TiO_2 in the gold electrolyte. Effects of the TiO_2 content on surface morphology, crystalline structure and microstructure of the composite film are investigated. Mechanical properties of the Au–TiO_2 composite films are evaluated by micro-Vickers hardness and micro-compression tests. The hardness increases from 135 to 207 H_V when the TiO_2 content is increased from 0 to 2.72 wt%. Specimens used in the micro-compression test are micro-pillars fabricated from the composite film, and the yield strength reaches 0.84 GPa by incorporating 2.72 wt% TiO_2 into the film.

Keywords: co-electrodeposition; Au–TiO_2 composite; oxide dispersion strengthening; micro-compression test

1. Introduction

Electrodeposition methods are widely applied in fabrication of micro-components used in miniaturized electronic devices such as microelectromechanical system (MEMS) devices. For instance, the proof mass and micro-springs in a highly-sensitive MEMS accelerometers are prepared by Au electrodeposition [1,2]. Au is used here because performance of a MEMS accelerometer is highly dependent on overall mass of the movable components, while miniaturization of the component is also required. Hence, Au (mass density = 19.32 g/cm^3 at 298 K) becomes the ideal material to achieve requirements of high performance and miniaturization at the same time. On the other hand, Au has relatively weak mechanical strengths among materials commonly used in electronics, and this raises a concern on the structure stability of movable micro-structures composed of Au. Strengthening of the electrodeposited Au becomes an important task to ensure high structure stability of the movable micro-structures.

Co-electrodeposition of metal matrix composites (MMCs) is an effective and simple strategy to enhance a specific property of electrodeposited materials. Common reinforcement materials are nanoparticles (NPs) include oxides such as Al_2O_3 [3], TiO_2 [4,5], and Cr_2O_3 [6], carbides like SiC [7] or graphitic materials like carbon nanofiber [8] and carbon nanotube [9], inorganic particles like phosphorus [10] and polymers like polyaniline [11]. For enhancing mechanical properties of electrodeposited Au while keeping the high mass density, the effects of oxide dispersion

strengthening [12] could be readily applied by incorporating a small amount of oxide NPs into the electrodeposited film.

In this study, TiO_2 NPs are introduced into the Au matrix composite by co-electrodeposition. Moreover, in consideration of the sample size effect [13], that is mechanical properties of metallic materials varied along with dimensions of the specimen used in the evaluation, the mechanical properties are evaluated by micro-compression test for application in miniaturized electronic devices.

2. Materials and Methods

Co-Electrodeposition of Au–TiO_2 Composite Films

The base electrolyte was a non-cyanide sulfite-based commercial Au plating bath purchased from MATEX·JAPAN Co., Ltd., Shizuoka, Japan. The bath was composed of 18.13 g/L of $Au(SO_3)_2$ and additives including ethylenediaminetetraacetic acid (EDTA) and sodium gluconate with pH value of 7.5. 10, 30, and 50 g/L of TiO_2 NPs (AEROXIDE® TiO_2 P25, Evonik, Essen, Germany) were added into the base electrolyte to form Au–TiO_2 composite films with different TiO_2 contents. Cold-worked Cu plates were masked with polyimide tape into a single side with surface area of 10×10 mm^2 as the working electrodes. Cu electrodes were treated with 1 M KOH and 1 M HCl for 1 min each at room temperature right before the electrodeposition. The counter electrode was a Pt plate with a total surface area of 40×10 mm^2, and the reference electrode was Ag/AgCl(sat. KCl). The electrodeposition was conducted at 5 mA/cm^2 using a potentiostat (1287A, Solartron, Leicester, UK). The TiO_2 contained electrolyte was ultrasonicated for 30 min using a ultrasonicator (VS-100III, AS ONE, Osaka, Japan) right before the deposition to improve the dispersion of TiO_2 NPs in the electrolyte. Temperature of the electrolyte was kept at 40 °C during the whole electrodeposition process.

Surface morphology of the films was observed with a scanning electron microscope (SEM, S-4300 SE, Hitachi, Tokyo, Japan). The composition was determined by the energy dispersive X-ray analyzer (EDX, EMAX EX-250, Horiba, Kyoto, Japan) equipped in the SEM. The crystal structure was characterized through an X-ray diffractometer (XRD, Ultima IV, Rigaku, Tokyo, Japan).

Mechanical properties of the films were appraised by a micro-Vickers hardness testing machine (HMV-G20s, Shimadzu, Kyoto, Japan) at 50 g of load and micro-compression evaluation using a lab-designed micro-testing system. Specimens used in the micro-compression tests had a cuboidal pillar shape with dimensions of 20 μm in height and 10×10 μm^2 square cross-section. The focus ion beam system (FIB, FB2100, Hitachi, Tokyo, Japan) was used to fabricate the micro-pillars. The pillar surface was further polished with low current Ga^+ beams to allow observation of the microstructure through a scanning ion microscope (SIM) equipped in the FIB.

Micro-compression tests were conducted using a flat-topped indenter with a diameter of 50 μm on the top surface. Load resolution of this equipment was 10 μN, and the displacement resolution was 5 nm. More details of the micro-testing system are reported in a previous study [14]. A constant displacement rate of 0.05 μm/s was used in all micro-compression tests.

3. Results

3.1. Surface Morphology and Crystalline Structure

TiO_2 concentration in the film was estimated from the proportion of Ti in the film by the EDX, which Ti signals detected by the EDX were assumed to be contributed by the TiO_2 NPs only. From the estimation, TiO_2 concentrations in films electrodeposited using the Au base electrolyte containing 0, 10, 30 and 50 g/L of the TiO_2 NPs were 0, 1.45, 1.69, and 2.72 wt% TiO_2 NPs, respectively. Surface morphology of the films are shown in Figure 1. Condensed structures were observed on surface of the pure Au film. Surfaces of the Au–TiO_2 composite films were composed of nodule structures, which were different from that of the pure Au film. The difference is suggested to be originated from the applied potential to the working electrode, since galvanostatic electrodeposition was applied here

and the electrical conductivity of TiO_2 is lower than that of Au, then incorporation of TiO_2 into the electrodeposited film would change the applied potential and eventually affect the nucleation of Au on the surface. In addition, TiO_2 NPs adsorbed on the surface could also promote heterogeneous nucleation of Au. Hence, nodule structures were observed and size of the nodule visibly reduced due to the promoted Au nucleation.

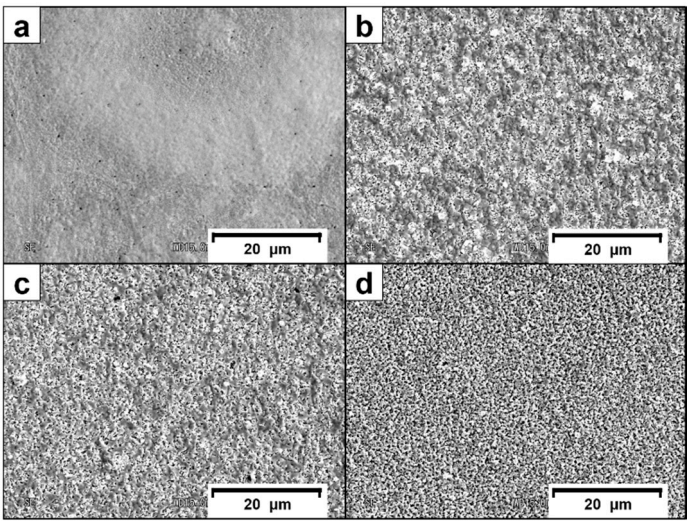

Figure 1. Surface morphology of electrodeposited (**a**) Au film and Au–TiO_2 composite films containing (**b**) 1.45, (**c**) 1.69, and (**d**) 2.72 wt% TiO_2.

XRD spectra of the TiO_2 NPs, pure Au and Au–TiO_2 composite films (2.72 wt% TiO_2) are shown in Figure 2. Typical face-centered cubic (FCC) Au characteristic peaks were identified in both Au and Au–TiO_2 composite films. The anatase TiO_2 (101) peak at $2\theta = 25.1°$ also appeared in XRD patterns of the Au–TiO_2 composite film containing 2.72 wt% TiO_2 (inset of Figure 2). This result confirmed incorporation of TiO_2 NPs into the Au matrix, forming a Au–TiO_2 MMCs film. In addition, the peak intensity ratio of FCC-Au (111) peak to other peaks was lower for the Au–TiO_2 composite film when compared with the pure gold film. This result again revealed the promoted heterogeneous nucleation of Au after adsorption of TiO_2 NPs on surface of the working electrode, because (111) orientation is the preferred nucleation orientation for Au and the intensity reduced when the heterogeneous nucleation is promoted.

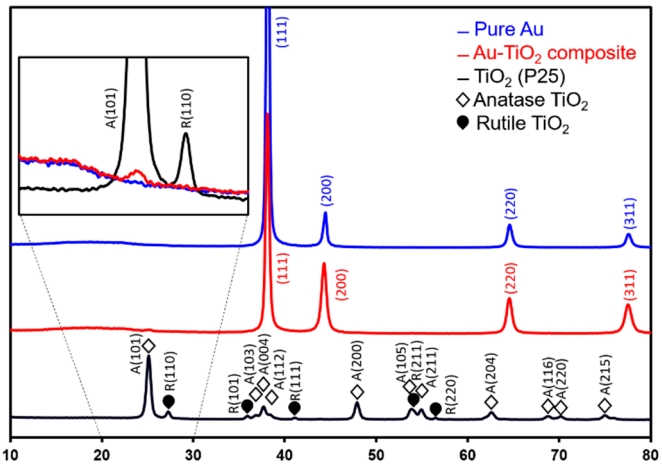

Figure 2. XRD spectra of Au, TiO_2 NPs, and the Au–TiO_2 composite film. The inset shows zoomed spectra of $2\theta = 20°$ to $30°$.

Average grain size of Au in the film was evaluated by averaging the weighted grain size values of primary (111) to quaternary (311) X-ray diffraction peaks from the Scherrer equation. The Scherrer equation is defined as follows:

$$\tau = \frac{K\lambda}{D\cos\theta} \quad (1)$$

where τ is the mean size of the ordered domain, K is the shape factor, λ is the wave length of incident X-ray beam (approximate to be 1.54×10^{-10} m), D is the full width at half maximum of the diffraction peak, and θ is the Bragg diffraction angle.

Average grain size of Au in the film without TiO_2 NPs was 20.4 nm while that of the 2.72 wt% TiO_2 Au–TiO_2 composite film was 16.3 nm. The decrease in the average grain size indicated grain refinement caused by incorporation of the TiO_2 NPs, which demonstrated the effect of promoted Au nucleation when adding TiO_2 NPs into the electrolyte.

Figure 3 shows microstructure of the electrodeposited films from SIM images of the as-fabricated micro-pillars. White spots on surface of the micro-pillars illustrated the portion that is TiO_2-rich (Figure 3b–d). Total amount of the TiO_2-rich portion increased with an increase in TiO_2 content in the micro-pillar.

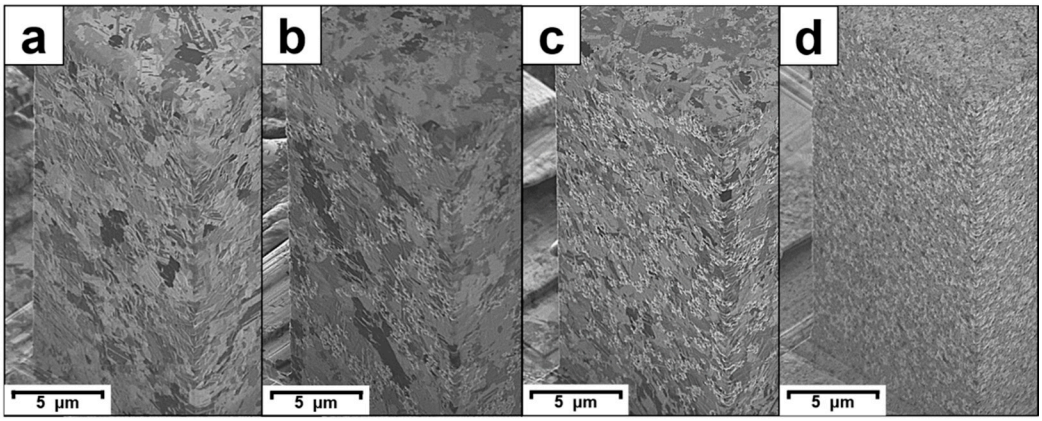

Figure 3. Scanning ion microscope (SIM) images showing microstructure of the (**a**) Au micro-pillars and Au–TiO_2 composite micro-pillars containing (**b**) 1.45, (**c**) 1.69, and (**d**) 2.72 wt% of TiO_2.

3.2. Mechanical Properties of Au–TiO_2 Composite

All micro-pillars showed ductile deformation and deformed to a barrel-shape after the micro-compression test. Figure 4 shows SIM images of the 2.72 wt% TiO_2 Au–TiO_2 composite micro-pillar before and after the micro-compression test. This deformation behavior is typical for micro-pillars composed of polycrystals [15].

Yield strengths (σ_y) of the micro-pillars were obtained from the engineering strain–stress curves shown in Figure 5. Micro-Vickers hardness (HV), σ_y, HV to σ_y coefficient (HV/σ_y), and theoretical mass density of the composites are summarized in Table 1. Theoretical mass density of the films was calculated from the TiO_2 NPs content and densities of pure Au and TiO_2. The HV increased from 135 to 207 HV, and the σ_y increased from 0.44 to 0.84 GPa due to its having 2.72 wt% of TiO_2 in the Au matrix. The strengthening was mostly contributed by the oxide dispersion strengthening. The HV/σ_y's were all close to three, and the ratio decreased as the σ_y increased. The HV/σ_y is commonly known as the Tabor factor. The value and the decreasing trend observed in this study both corresponded well with the behavior of close-packed structure metals reported in the literature [16]. Mass density of 2.72 wt% TiO_2 content Au–TiO_2 composite was 98% of that pure Au while the σ_y increased by almost 91%.

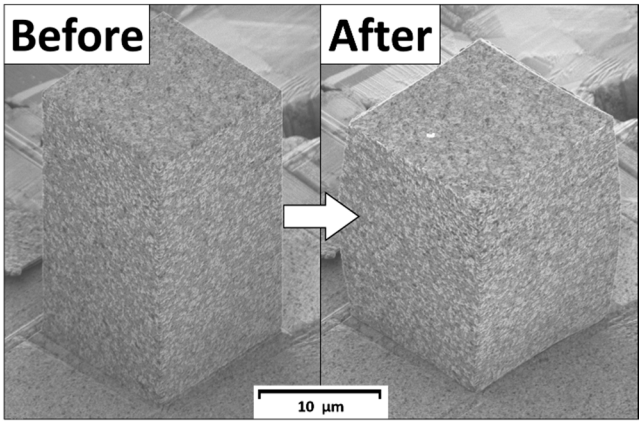

Figure 4. SIM images of the Au–TiO_2 (2.72 wt%) micro-pillar before and after the micro-compression test.

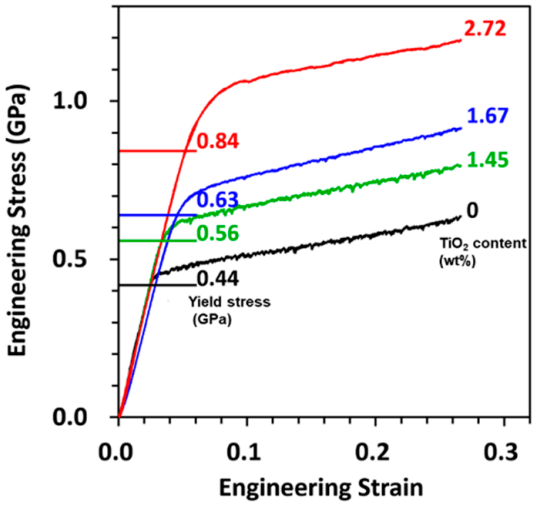

Figure 5. Engineering strain–stress curves of all micro-pillars.

Table 1. TiO_2 content, micro-Vickers hardness (HV), yield strength (σ_y), HV to σ_y coefficient (HV/σ_y), and mass density of the pure Au and Au–TiO_2 composite films.

Electrolyte	TiO_2 Content (wt%)	HV (Hv)	σ_y (GPa)	HV/σ_y	Mass Density (g/cm^3)
0 g/L TiO_2	-	135	0.44	3.01	19.32
10 g/L TiO_2	1.45	162	0.56	2.84	19.08
30 g/L TiO_2	1.67	176	0.63	2.74	19.05
50 g/L TiO_2	2.72	207	0.84	2.42	18.90

4. Conclusions

In this work, Au–TiO_2 composite films were fabricated by the co-electrodeposition method, and the mechanical properties were evaluated by micro-Vickers hardness and micro-compression tests. XRD spectrum of the films indicated grain refinement in the electrodeposited Au after incorporation of TiO_2 NPs into the film. Vickers hardness of the Au-based film was enhanced from 135 to 207 Hv by incorporating 2.72 wt% of TiO_2 into the film, and yield strength of the micro-pillar reached 0.84 GPa. The yield strength was improved by ~91% and the mass density reduced by only ~2% when compared with those of pure gold. In conclusion, the Au–TiO_2 composite possesses high strength with high mass density, which is promising for miniaturized electronic devices requiring low Brownian noise with high structure stability.

Author Contributions: Conceptualization, Y.-A.C., T.-F.M.C. and M.S.; Methodology, Y.-A.C., T.-F.M.C.; Validation, C.-Y.C., D.Y., H.I.; Formal analysis, Y.-A.C., C.-Y.C.; Investigation, Y.-A.C.; Resources, M.S.; Data curation, Y.-A.C.; Writing—original draft preparation, Y.-A.C.; Writing—review and editing, Y.-A.C., T.-F.M.C., M.S.; Visualization, Y.-A.C.; Supervision, T.-F.M.C. and M.S.; Project administration, K.M. (Katsuyuki Machida) and M.S.; Funding acquisition, K.M. (Kazuya Masu) and M.S. All authors have read and agreed to the published version of the manuscript.

Funding: This research was funded by the New Energy and Industrial Technology Development Organization (NEDO), and is supported by JST CREST Grant Number JPMJCR1433.

Conflicts of Interest: On behalf of all of the co-authors, the corresponding author states that there is no conflict of interest.

References

1. Yamane, D.; Konishi, T.; Matsushima, T.; Machida, K.; Toshiyoshi, H.; Masu, K. Design of sub-1g microelectromechanical systems accelerometers. *Appl. Phys.* **2014**, *104*, 074102. [CrossRef]
2. Masu, K.; Machida, K.; Yamane, D.; Ito, H.; Ishihara, N.; Chang, T.F.M.; Sone, M.; Shigeyama, R.; Ogata, T.; Miyake, Y. CMOS-MEMS based microgravity sensor and its application. *ECS Trans.* **2020**, *97*, 91–108. [CrossRef]
3. Chiu, S.Y.; Chung, S.T.; Lin, C.Y.; Tsai, W.T. Electrodeposition of Ni-Al_2O_3 composite coatings employing supercritical CO_2 baths. *Surf. Coat. Technol.* **2014**, *247*, 68–73. [CrossRef]
4. Imbaby, M.F.; Jiang, K. Stainless steel–titania composite micro gear fabricated by soft moulding and dispersing technique. *Microelectron. Eng.* **2010**, *87*, 1650–1654. [CrossRef]
5. Parida, G.; Chaira, D.; Chopkar, M.; Basu, A. Synthesis and characterization of Ni-TiO_2 composite coatings by electro-co-deposition. *Surf. Coat. Technol.* **2011**, *205*, 4871–4879. [CrossRef]
6. Srivastava, M.; Balaraju, J.N.; Ravishankar, B.; Rajam, K.S. Improvement in the properties of nickel by nano-Cr_2O_3 incorporation. *Surf. Coat. Technol.* **2010**, *205*, 66–75. [CrossRef]
7. Maurin, G.; Lavanant, A. Electrodeposition of nickel/silicon carbide composite coatings on a rotating disc electrode. *J. Appl. Electrochem.* **1995**, *25*, 1113–1121. [CrossRef]
8. Arai, S.; Endo, M. Carbon nanofiber–copper composite powder prepared by electrodeposition. *Electrochem. Commun.* **2003**, *5*, 797–799. [CrossRef]
9. Arai, S.; Saito, T.; Endo, M. Cu–MWCNT composite films fabricated by electrodeposition. *J. Electrochem. Soc.* **2010**, *157*, D147–D153. [CrossRef]
10. Graydon, J.W.; Kirk, D.W. Suspension Electrodeposition of Phosphorus and Copper. *J. Electrochem. Soc.* **1990**, *137*, 2061–2066. [CrossRef]
11. Hu, C.C.; Chen, E.; Lin, J.Y. Capacitive and textural characteristics of polyaniline-platinum composite films. *Electrochim. Acta* **2002**, *47*, 2741–2749. [CrossRef]
12. Ibrahim, I.A.; Mohamed, F.A.; Lavernia, E.J. Particulate reinforced metal matrix composites—A review. *J. Mater. Sci.* **1991**, *26*, 1137–1156. [CrossRef]
13. Greer, J.R.; Oliver, W.C.; Nix, W.D. Size dependence of mechanical properties of gold at the micron scale in the absence of strain gradients. *Acta Mater.* **2005**, *53*, 1821–1830. [CrossRef]
14. Takashima, K.; Higo, Y.; Sugiura, S.; Shimojo, M. Fatigue crack growth behavior of micro-sized specimens prepared from an electroless plated Ni-P amorphous alloy thin film. *Mater. Trans.* **2001**, *42*, 68–73. [CrossRef]
15. Chen, C.Y.; Yoshiba, M.; Nagoshi, T.; Chang, T.F.M.; Yamane, D.; Machida, K.; Masu, K.; Sone, M. Pulse electroplating of ultra-fine grained Au films with high compressive strength. *Electrochem. Commun.* **2016**, *67*, 51–54. [CrossRef]
16. Zhang, P.; Li, S.X.; Zhang, Z.F. General relationship between strength and hardness. *Mater. Sci. Eng. A* **2011**, *529*, 62–73. [CrossRef]